

# A wavelet approach to the short-term to pluri-decennial variability of streamflow in the Mississippi river basin from 1934 to 1998

N. Massei,<sup>a\*</sup> B. Laignel,<sup>a</sup> E. Rosero,<sup>b</sup> A. Motelay-massei,<sup>a</sup> J. Deloffre,<sup>a</sup> Z.-L. Yang<sup>b</sup>  
and A. Rossi<sup>a</sup>

<sup>a</sup> UMR CNRS 6143 “Continental and Coastal Morphodynamics”, Department of Geology, University of Rouen, 76821 Mont-Saint-Aignan Cedex, France

<sup>b</sup> Department of Geological Sciences, The University of Texas at Austin, 1 University Station #C1100 Austin, TX 78712-0254, USA

**ABSTRACT:** The temporal variability of streamflow in the Mississippi river basin, including its major tributaries (Missouri, Upper Mississippi, Ohio and Arkansas rivers), was analysed using continuous wavelet methods in order to detect possible changes over the past 60 years. Long- to short-term fluctuations were investigated. The results were compared with SOI, PDO and NAO indices and precipitation time series and were also processed by wavelet methods. A major change point around 1970, also reported in other works, was recovered in all climate and hydrological processes. It is characterised by the occurrence of an 8–16-year mode for Upper Mississippi and Missouri and of a 3–6-year mode for all rivers. Two other discontinuities around the mid-1950s and 1985 were also detected. A strong power attenuation of the annual cycle in the Arkansas, Upper Mississippi and Missouri rivers was also found between 1955 and 1975. In general, the dominant modes of inter-annual to pluri-annual streamflow variability lay in the 2–4-year, 4–8-year and 10–16-year ranges, which was typical of SOI for the period of study. A preferential link with the Mississippi basin headwater zone (i.e. Upper Mississippi and Missouri) was deduced during the  $\approx 1934$ –1950 and  $\approx 1970$ –1985 periods.

Overall, the contribution of inter-annual to pluri-annual oscillations ranged from 6.6 to 26% of streamflow variance, while the short-term scales (<2–3 weeks) explained from 1.1 to 6.4%. The annual cyclicality explained from 19.1 to 48.6% of streamflow variance. High-frequency streamflow fluctuations linked to synoptic activity were also found to increase after 1955 for all basins except Upper and Lower Mississippi, apparently modulated by a  $\approx 2$ –4-yr oscillation. Copyright © 2010 Royal Meteorological Society

KEY WORDS Mississippi; streamflow variability; climate fluctuations; wavelet

Received 5 October 2007; Revised 29 June 2009; Accepted 10 July 2009

## 1. Introduction

Great rivers' watersheds play a major role in the world in terms of water resources. However, the way climate and global environmental changes affect streamflow variability in such basins remains challenging, especially in terms of quantification of their respective impact. Ziegler *et al.* (2005) stated that about 350 years are required to detect plausible changes in the annual streamflow. Yet, it is still possible to attempt the description of changes in streamflow during shorter periods (measurements usually do not span more than 100 years).

In the conterminous or in the central United States, many authors investigated the temporal trends of streamflow variability (Lins and Slack, 1999; McCabe and Wolock, 2002). To investigate the temporal trends in streamflow in the United States, Lins and Slack (1999)

used a methodology based on compilation of quite a large number of daily discharge records (i.e. 395 time series) for watersheds relatively free of anthropogenic effects by trend testing. These authors detected increasing trends for most of the US water resource regions for discharge regimes below the upper quartile (Q75), except on the Pacific coast and in some regions of the Southeast, which exhibited decreasing trends at all quantiles. They concluded that the conterminous United States was getting wetter, but it was less extreme.

Pagano and Garen (2005), in their study of streamflow data from 141 unregulated basins in the western United States, reported three different periods of streamflow variability: (1) a low variability and high persistence (i.e. positive autocorrelation, which means that either dry or wet periods follow each other) between the 1930s and the 1950s, (2) a low variability and anti-persistence (dry periods more often followed by wet periods and converse) between the 1950s and the 1970s and (3) a high variability and persistence after the 1980s. After McCabe *et al.* (2004), 52% of the spatial and temporal variance in

\*Correspondence to: N. Massei, UMR CNRS 6143 “Continental and Coastal Morphodynamics”, Department of Geology, University of Rouen, 76821 Mont-Saint-Aignan Cedex, France.  
E-mail: nicolas.massei@univ-rouen.fr

multi-decadal drought frequency over the United States may be attributed to the PDO and the Atlantic multi-decadal oscillation (AMO), while an additional 22% could be possibly due to general climate warming.

McCabe and Wolock (2002) carried out a study on large-scale streamflow variability using the records of several tens of gauges and concluded that there is a step increase in streamflow variability rather than a gradual change around 1970. Coulibaly and Burn (2004) also noted striking climate-related features before the 1950s and after the 1970s in mean annual streamflows from 79 rivers selected from the Canadian Reference Hydrometric Basin Network (RHBN) by continuous wavelet transform. This 1970 change point was also reported in the study from Anctil and Coulibaly (2004) on the description of the local inter-annual streamflow variability in southern Québec, Canada.

Recent works published on the Mississippi basin attempted to predict the potential effects of climate changes on hydrology (Nijssen *et al.*, 2001; Jha *et al.*, 2004, 2006): for instance, Nijssen *et al.* (2001), modelling water balance changes up to 2045, demonstrated a decrease in snow water storage, resulting in increased runoff during the winter, but decreased runoff during the snowmelt period. Many significant works used trend-testing statistical methods to detect potential changes in both amplitude and mean values (Lins and Slack, 1999; maugé, 2004; Novotny and Stefan, 2007). In other words, these works aim at describing and quantifying potential temporal changes in mean and amplitude in streamflow. This addresses the problem of non-stationarity for which wavelet-based methods are precisely designed.

In this work, we propose to investigate streamflow variability in the Mississippi river basin using continuous wavelet analysis. This method had apparently never been applied to Mississippi streamflow according to the very rich literature available. The paper aims at giving a quantitative overview, statistically speaking, of the respective contribution of long-term potentially climate-related oscillations. Two main issues are addressed: (1) the identification of the nature of time-varying characteristics of long-term fluctuations and the quantification of their influence in streamflow variability and (2) the evolution of short-term fluctuations (1 day to 3 weeks) and their potential link to longer-term climate patterns. Daily streamflow data of some of the major tributaries of the

Mississippi river are used, that is, Missouri, Upper Mississippi, Ohio and Arkansas rivers. These streamflow series are finally compared with the global Mississippi streamflow series.

## 2. Hydroclimatological data

### 2.1. Hydrometeorological time series

The discharge time series that was used consisted of daily streamflow values from the entire Mississippi river watershed (referred to as 'Lower Mississippi') and some of its most significant sub-basins in terms of discharge contribution, i.e. Arkansas, Ohio, Upper Mississippi and Missouri Rivers (Figure 1a and b). Overall, five daily streamflow time series were used. Data were obtained from the National Water Information System of the US Geological Survey (<http://waterdata.usgs.gov/nwis/sw>). All the records used here span a 64-year period from 1934 to 1998. Streamflow values were recorded from stations located at the outlet of the Missouri, Upper Mississippi, Ohio and Arkansas Rivers. There were very few missing values; when existing, blanks were interpolated using a cubic spline algorithm. The overall Mississippi streamflow time series was also investigated, corresponding to daily values at the outlet of the Lower Mississippi. Table I gives the location of stream gauges along with the total watershed area for each basin and the number of large dams when available.

Precipitation variations were also investigated. The series that was used consisted of mean annual precipitation data for climatic regions of the United States (Figure 1a) between 1895 and 2000, as defined in Guttman and Quayle (1996) and provided by the US National Climatic Data Center (NCDC). The climatic regions selected for data analysis were – according to each basin – the West North Central, East North Central, Central and South regions. An additional mean precipitation series was used by averaging over five others to represent precipitation over all five regions. Although this only gives a simplistic representation, it is likely to be sufficient in order to look at large-scale long-term modes of variability in precipitation of annual rainfall in the whole area.

### 2.2. Climate index time series

Additionally, three monthly climate indices, among major indicators, were chosen according to the pertinence of

Table I. Stream gauges location and total area and number of large dams for all basins.

	Lower Mississippi	Arkansas	Ohio	Upper Mississippi	Missouri
Watershed area (km <sup>2</sup> )	3 202 230	435 122	490 603	489 508	1 331 810
Stream gauge location	Tarbert+RR landings (LA)	Murray dam near Little Rock (AR)	Metropolis (IL)	Saint Louis (MO)	Hermann (MO)
Large Dams (World Resources Institute)	2091	387	711	Unknown	581

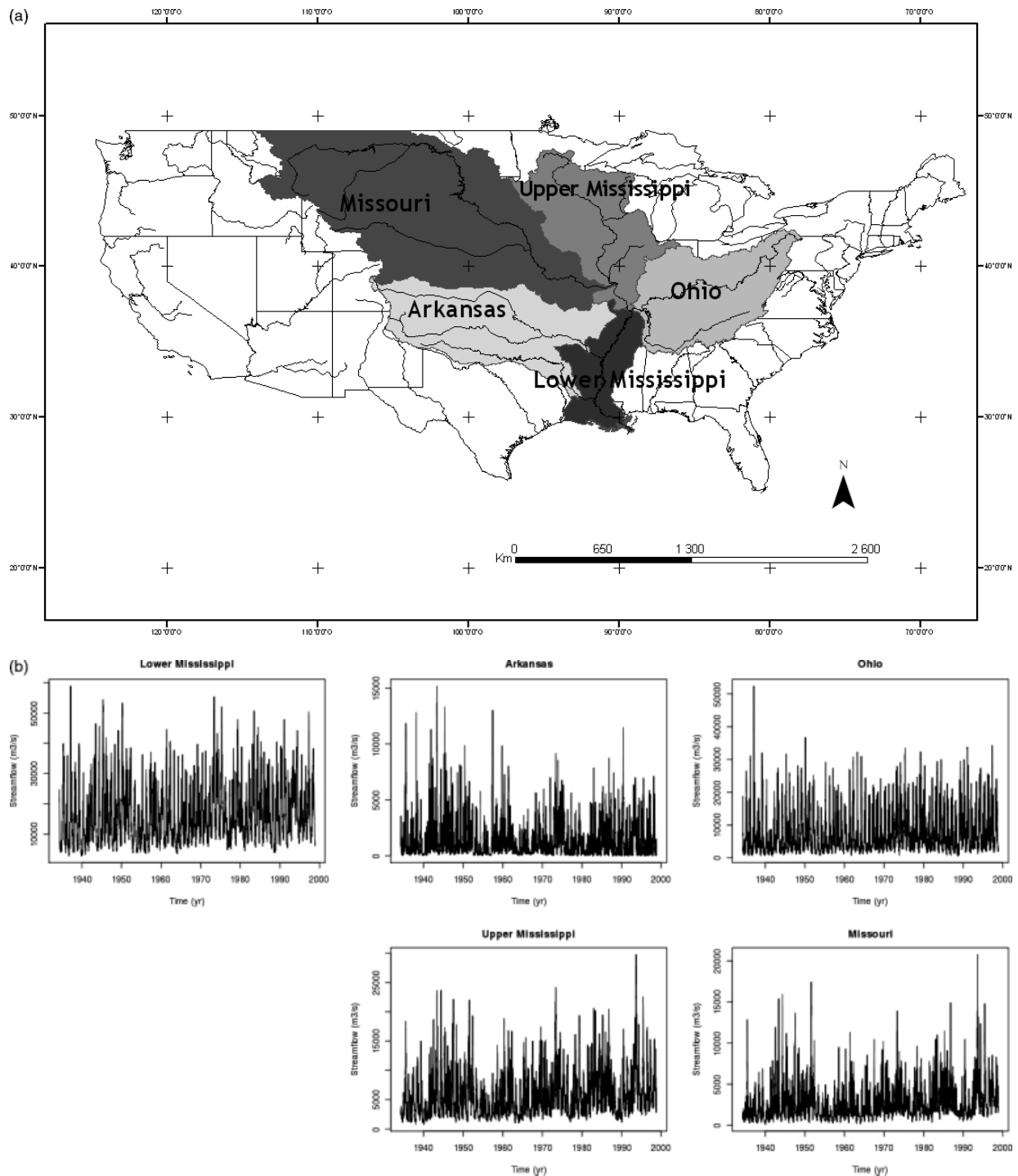


Figure 1. (a) The Mississippi river basin and its main tributaries: the bottom left map shows the regional precipitation regions defined in Guttman and Quayle (1996); (b) daily streamflow time series used for the study.

their effect on hydro-climatic variability in North America (Jain and Lall, 2001; Anctil and Coulibaly, 2004; Coulibaly and Burn, 2004; Pagano and Garen, 2005; Stewart *et al.*, 2005): the Pacific decadal oscillation (PDO), the Southern oscillation (SO) and the North Atlantic oscillation (NAO). These three climate indices are obviously not the only climate patterns or teleconnections influencing streamflow and, to a larger extent, hydroclimatology of the United States. However, they are still major indicators of climate variability and changes in

the Northern Hemisphere and North America. As a consequence, the main characteristics affecting their variability are likely to be representative of major global climate activity in the Mississippi basin. Their temporal variability may then constitute a good indicator of some general relationships between climate fluctuations and streamflow variability.

The PDO is a long-lived El Niño-like pattern of Pacific climate variability, which can be defined as the leading principal component of North Pacific monthly sea surface

temperature variability. As reported in Hanson *et al.* (2006), a change in the PDO index is a change in the cold and warm water masses of the Pacific Ocean and alters the path of the jet stream that delivers storms to the United States. A positive-phase PDO acts to push the jet stream further south into the southwestern United States, while a negative-phase PDO brings the jet stream further north. Therefore, a negative-phase PDO index may lead to less precipitation in the southwest.

The Southern Oscillation index (SOI) is calculated from the monthly or seasonal fluctuations in the air pressure difference between Tahiti (T) and Darwin (D) (i.e. mean sea level pressure anomalies  $T - D$ ). Sustained negative values of the SOI often indicate El Niño episodes; the SOI and El Niño/Southern oscillation (ENSO) are out of phase. During El Niño years/negative SOI, the storm track splits more frequently into two preferred branches. The first branch would bring mildly increased storminess in the southern coast of the main part of Alaska. On the contrary, the second branch would involve a weakening of the storms approaching the Pacific northwest and southwest Canada. In this last case, winter tends to be wetter than usual from southern California eastward across Arizona, southern Nevada and Utah, New Mexico and into Texas. In the Pacific northwest, El Niño tends to bring drier winters in areas including Washington, Oregon and the more mountainous portions of Idaho, western Montana and northwest Wyoming; these areas correspond well to the northwestern part of the Missouri River. In between these regions, including central and northern California, northern Nevada, southern Oregon, northern Utah, southern Wyoming and much of Colorado, the effects of El Niño are ambiguous. No strong association can be discerned in either direction (towards wet or dry).

As described by Hurrell (2000), 'The NAO refers to a redistribution of atmospheric mass between the Arctic and the subtropical Atlantic, and swings from one phase to another produce large changes in the mean wind speed and direction over the Atlantic, the heat and moisture transport between the Atlantic and the neighboring continents, and the intensity and number of storms, their paths, and their weather'. The NAO reflects the main fluctuation of climatic conditions in Europe and also affects the eastern/north-eastern coast of North America: during positive NAO, these regions as well as northern Europe undergo wetter weather conditions and the converse is true for negative NAO.

The climate index data series can be obtained from a number of climate research centre websites (<http://www.cru.uea.ac.uk>, <http://www.cgd.ucar.edu/cas/jhurrell/indices.htm>, <http://jisao.washington.edu/pdo/PDO.latest>).

### 3. Methods

Data analysis consisted of Fourier spectral and continuous wavelet analyses. Fourier spectral analysis was used as a first step to describe the overall behaviour of each time series for the selected 64-year period.

Fourier energy spectra allowed identification of specific behaviours according to representative time scales, as well as the comparison of streamflow variability for each watershed. Spectra were obtained from autocorrelation functions of time series, on which fast Fourier transform were performed with application of a Tukey filtering window. Fourier spectra were used to compare the hydrological behaviour of the sub-basins: for any scaling field, the power or energy spectrum for a given time series has a power-law dependency on frequency:

$$E(\omega) \sim \omega^{-\beta} \quad (1)$$

where  $\omega$  is the frequency,  $\beta$  the spectral exponent and  $E(\omega)$  the energy of the spectrum. When plotted within a log–log scale, the energy spectrum displays a linear behaviour with slope equal to  $-\beta$ . A slope change in the spectrum separates different scaling fields, each related to a different hydrologic regime according to time scale. Here, the period ( $1/\omega$ ) is used for the  $x$ -axis instead of frequency.

Time–frequency exploration was performed in a second step using continuous wavelet transform; this method allows identification of instationarity of the time series studied. This approach has already been successfully applied to surface watersheds (Coulibaly and Burn, 2004; Labat *et al.*, 2005). Many published works have already presented the general principle of wavelet analysis (see, for instance, Anctil and Coulibaly, 2004; Labat, 2005), most of which are based on the very accurate presentation of continuous wavelet analysis techniques by Torrence and Compo (1998); the reader is referred to the above-mentioned paper. An even more detailed mathematical presentation is given in Schneider and Farge (2006). In our study, the Morlet wavelet (a Gaussian-modulated sine wave) was chosen for continuous wavelet transform owing to its good basic frequency resolution; in addition, a wavenumber of 6 was used for the reference mother wavelet resolution, which offered a good trade-off between spectral component detection and time localisation.

The question often arises about the choice of the mother wavelet (What if a different wavenumber/wavelet were chosen? Would the result be the same? etc.). Other wavelets can be used and have been tested to analyse the present dataset, namely the Paul and DOG (derivative of Gaussian). Depending on the wavelet used, different types of features show up slightly differently. This does not dramatically change the characteristics of the spectral content: some features appear more clearly than others when a given wavelet/wavenumber is used, and the converse is also true. Ideally, several wavelet and several basic resolutions of the mother wavelet (wavenumber) should be employed to highlight the most striking features of a signal and to choose the most appropriate tool regarding the phenomenon to be analysed and described. For instance, increasing the magnitude of the wavenumber would result in a better frequency resolution, in the detriment of time resolution, i.e. the

temporal discontinuities would get ‘blurred’. All these tests were realised in this study.

The time–frequency diagrams produced give a visualisation of the main energy bands present in the time series and highlight instationarities, that is, the temporal discontinuities that may exist in the signal studied. Finally, examination of power fluctuations for either the entire spectral content or selected energy bands is carried out by computing and plotting the so-called scale-averaged continuous wavelet spectra. The scale-averaged wavelet power corresponds to the temporal evolution of power associated with a selected band of the wavelet spectrum.

**4. Scaling regimes of streamflow time series**

As a preliminary step to the identification of characteristic time scales and time periods, Fourier spectral analysis is applied to each time series. Table II summarises the

main results that could be obtained from autocorrelation functions and corresponding energy spectra (Figure 2).

For all streamflow series, trends (to be removed before autocorrelation and Fourier transform) were statistically tested. All streamflow time series exhibited increasing trends and the F-statistic provided indication on the increase rate of each trend. Contrary to what Walling and Fang (2003) stated, an increasing trend for the Mississippi River was found to be statistically significant at the 95% confidence limit ( $F = 392.4, p < 0.0001$  in Table II).

Autocorrelation functions (Figure 2) clearly show that the annual cycle is well represented in the series. Indeed, autocorrelation functions display a strong periodicity (gain in correlation) every  $\sim 365$  days. However, they also reveal different memory effects, which can be represented as a quantitative value characterising the degree of linear correlation for a value with the previous ones. Here, the memory effect is estimated by fitting an exponential decay ( $y = y_0 + a.e^{-b.t}$ ) to the autocorrelograms. The

Table II. Trends, representative time scales and slopes (exponents) for the different streamflow series over the 64-year (1934–1998) period.

	Lower Mississippi	Arkansas	Ohio	Upper Mississippi	Missouri
F-statistic for increasing trend in streamflow	392.4	115.5	228.4	986.2	906.6
Memory effect (per day)	$-2.64 \cdot 10^{-2}$	$-2.98 \cdot 10^{-2}$	$-2.70 \cdot 10^{-2}$	$-2.32 \cdot 10^{-2}$	$-2.26 \cdot 10^{-2}$
Breakup time scale (day)	37	15	32	11	14
$\beta_1$ exponent	8.02	6.32	6.13	7.21	7.21
$\beta_2$ exponent	2.08	2.78	1.56	3.04	2.32

All  $p$ -values are  $<0.0001$ .

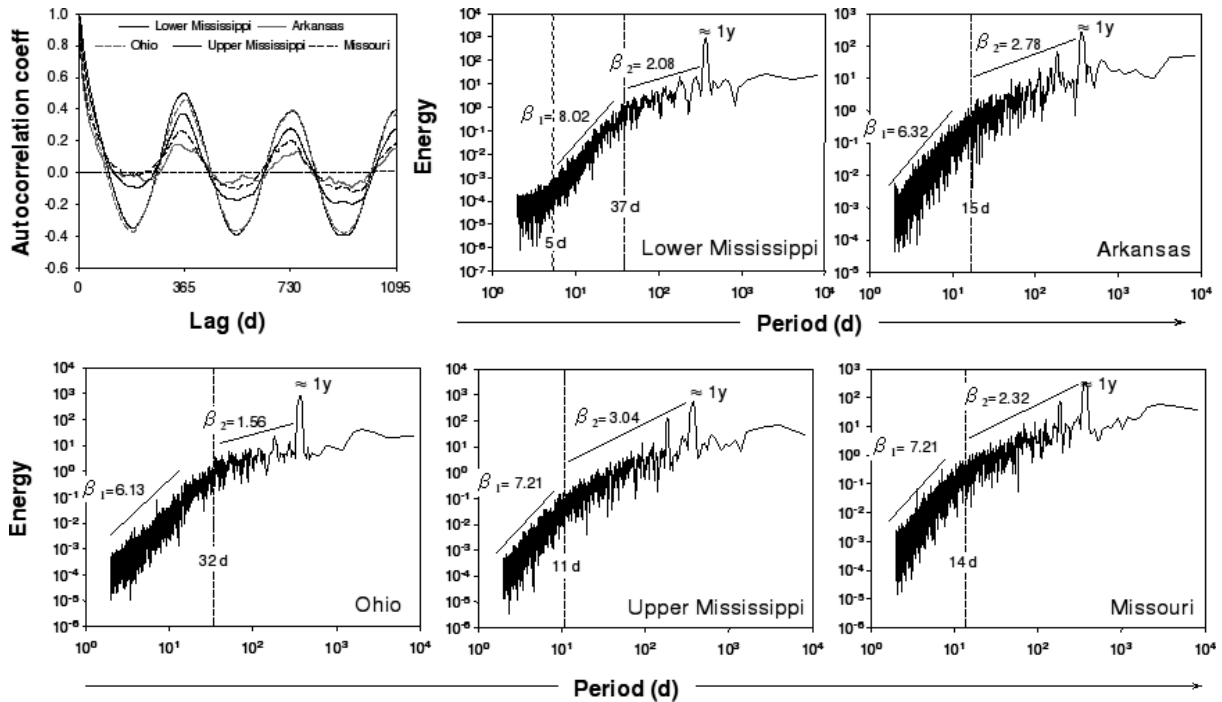


Figure 2. Autocorrelation functions and Fourier energy spectra of streamflow time series. Each spectrum displays two different scaling regimes separated by an 11–37-day time scale, which characterises the difference between short-term behaviour (mainly related to the meteorologic conditions and physiographic features of each basin) and long-term climate patterns. This typical time scale can be related to the so-called synoptic maximum.

speed at which the fitted exponential decays (expressed in per day) characterises the speed at which information gets lost in the time series. It constitutes an indicator of the global structuration of a time series. The memory effect values presented in Table II correspond to the values of parameter  $b$  of the exponential. The smaller the value of  $b$ , the smaller is the memory effect. Arkansas has the smallest memory effect, while Missouri displays the largest one: the Arkansas streamflow series would then be poorly structured regarding other watershed series. The reason why the Arkansas streamflow series is less structured overall than the others is not clear. Additional research and further investigation would be needed in order to provide consistent hypotheses for this special behaviour of Arkansas streamflow autocorrelation. In all of the events, the autocorrelation function remains an interesting tool to get an overview of the general behaviour of a signal, although it only provides global information precisely.

Representative time scales and scaling regimes could be investigated by Fourier spectral analysis (Figure 2). The spectra display clear breaks separating at least two distinct flowing regimes. The values of the associated spectral exponents  $\beta$  are related to the variability of each signal according to time scale: the lower the magnitude of  $\beta$ , the higher is the variability in the data, whereas higher  $\beta$  values correspond to smoother variations. The two different slopes  $\beta_1$  and  $\beta_2$  characterise two types of flow regimes associated respectively with a short-term variability and a long-term variability, respectively. The breakup time scale that separates these two types of flowing regimes would be related to the typical time scale separating short-term meteorological field fluctuations from long-term climate oscillations. The Fourier period separating these two domains is known as *the synoptic maximum*, the maximum time scale characterising the lifetime duration of synoptic events. All energy spectra display a 1-year periodicity (the annual cycle) and are characterised by distinct  $\beta_1$  and  $\beta_2$  values, with slightly different synoptic maxima.

In the long term ( $\beta_2$  exponent), the Mississippi river sub-basins reveal different behaviours. The Upper Mississippi watershed displays a lower variability (highest  $\beta_2$  exponent) than the other sub-basins. On the contrary, Ohio is characterised by a higher variability in the long term (low  $\beta_2$  exponent of 1.56). In the short term, arranging the various basins according to decreasing  $\beta_1$  gives the following: Lower Mississippi, Missouri/Upper Mississippi, Arkansas, Ohio. Arkansas and Ohio present a high variability (low  $\beta_1$  exponents), whereas Upper Mississippi/Missouri show smoother variations (higher  $\beta_1$ ). Arkansas displays more contrasted scaling properties between the two long- and short-time scaling regimes with a low  $\beta_1$  and a high  $\beta_2$  exponent. The variability in the streamflow is high in the short term, while longer time scales exhibit a lower variability with smoother variations.

It is difficult to distinguish any clear hierarchisation of watersheds according to their scaling exponents. This

might be either due to the small amount of samples (i.e. the five watershed time series used) or due to the statistical nature of the scaling exponent  $\beta$ , inasmuch as the stochastic processes.

## 5. Fluctuations at annual to pluri-decennial scales

In this section, continuous wavelet transform (Figure 3) is used to investigate the variability of each streamflow series according to time (i.e. throughout the period of study) and wavelet scale (i.e. from the short term to the long term). The detected modes of variability are then compared with those characterising climate indices and precipitation.

Colours indicate the distribution of power, here expressed as normalised decibels (i.e. maximum power = 0 db for each scale), with a decreasing power from purple (maximum power) to dark red (minimum power). All series were zero-padded to twice the data length to prevent spectral leakage consequently to wavelet transform. However, zero-padding does not prevent from edge effects, causing some spectral components to be underestimated, especially in the lowest frequencies and near the edges of the series. The area under the white-dotted curve on each local wavelet spectrum marks those parts of the spectrum where energy bands are likely to be less powerful than they actually are. This area is known as *the cone of influence*.

### 5.1. Main modes of variability and characteristic time scales

Several energy bands can be separated on the streamflow local wavelet spectra (Figure 3, Table III):

- A 1-year band (annual cycle, A in Figure 3). A strong and obvious attenuation of the intensity – in terms of variance – of the annual cycle between approximately 1955 and 1975 is observed for all watersheds. This phenomenon is less marked for the Lower Mississippi and Ohio Rivers, which reveal a good sustenance of the annual cycle power. The annual cycle for Arkansas River seems poorly structured and less powerful.
- A 2–4-year band (B), a powerful structure that occurs around 1990 in all streamflow series except Ohio River, for which this band is barely present.
- A 5–8-year band (C), which seems to be affected by a change towards a 3–6-year band (D) around 1970.
- A 8–16-year band (E) clearly characterises the Upper Mississippi and Missouri Rivers, with a powerful structure beginning in the early 1970s (around a 10-year Fourier period). This structure is not visible in other streamflow series.
- A last low-frequency 12–16-year band (F) is only detected in the Lower Mississippi and Arkansas streamflow spectra, well localised between 1940 and the mid-1980s.

Common fluctuations could be recovered for all streamflow series, while others (for instance, the 8–16-year band E) seemed more specific for some watersheds

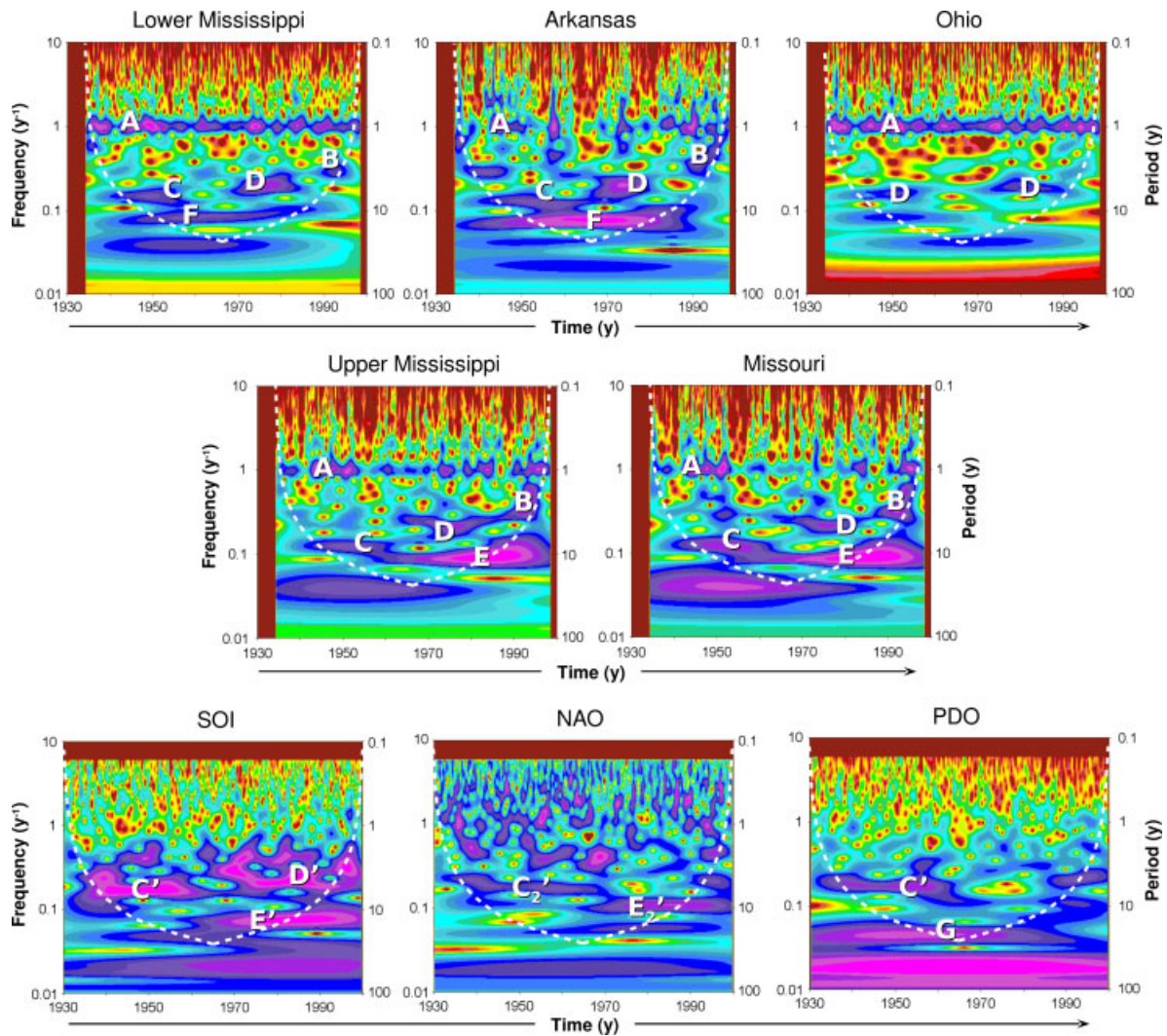


Figure 3. Continuous local wavelet spectra of streamflow and climate index time series. The white dotted curves delimit the cone of influence, i.e. the area under which power can be underestimated as a result of edge effects, wraparound effects and zero padding. This figure is available in colour online at [wileyonlinelibrary.com/journal/joc](http://wileyonlinelibrary.com/journal/joc)

Table III. Contribution of selected energy bands to total variance of streamflow for all studied basins.

Energy band	Streamflow	Energy band	PDO	SOI	NAO
A	1 year	G	20–26 years	–	–
B	2–4 years	C'	4–8 years	4–8 years	–
C	5–8 years	D'	–	2–8 years	–
D	3–6 years	E'	–	10–16 years	–
E	8–16 years	C <sub>2</sub> '	–	–	5–7 years
F	12–16 years	E <sub>2</sub> '	–	–	8–12 years

(typically Upper Mississippi and Missouri). In addition, a shift towards higher frequency fluctuations (Figure 3, in chronologic order: C->D->B) could be observed for almost all series but Ohio.

In brief, three major patterns show up on the local wavelet spectra (Figure 3):

1. A first discontinuity is visible around 1950–1960; it involves a shift from band C to D for Lower Mississippi, Arkansas, Upper Mississippi and Missouri and

an interruption of band D for Ohio. It is also accompanied by a lack of power affecting more specifically the annual band (A) between approximately 1950 and 1975 as described above, and seems more pronounced for Arkansas, Upper Mississippi and Missouri.

2. A second discontinuity is visible around 1970 and seems to affect most of the signal components. It is characterised by the occurrence of a powerful 8–16-year band (E) for both Upper Mississippi and

Missouri Rivers, and of a 3–6-year band (D) for all rivers.

3. A third discontinuity can be observed around 1985: the B and D energy bands seem to be more particularly concerned by this change, while the lower frequencies do not display any striking change. The 3–6-year band (D) would shift quite abruptly towards a 2–4-year fluctuation (B).

These results seem to be in concordance with those of Pagano and Garen (2005), who concluded that there exist three different periods of streamflow variability in their analysis of April–September streamflow volume data from 141 unregulated basins in the western United States: between the 1930s and the 1950s, the 1950s and the 1970s and after the 1980s. Similarly, Coulibaly and Burn (2004) reported strong local correlations between teleconnection patterns and western, central and eastern Canadian streamflows in both 2–3- and 3–6-year bands with striking changes around 1950 and 1970. Other authors, such as McCabe and Wolock (2002), reported a 1970 discontinuity, which they interpreted as a step increase in streamflow in the United States, coinciding with an increase in precipitation. Overall, these studies did not propose any physical mechanisms to explain the physical influence of climate over streamflow – which remains extremely difficult.

Wavelet transforms of monthly SOI, PDO and NAO indices were performed in order to compare the scale and temporal patterns of streamflow with the fluctuations of three of the major climatic patterns known to impact North America (Anctil and Coulibaly, 2004; Coulibaly and Burn, 2004; Hanson *et al.*, 2006). All three indices are affected by clear temporal discontinuities in their spectral composition (Figure 3). For the 1930–2000 period, the selected climate indices are characterised by the following modes:

- > SOI: before ~1970, 4–7-year band (C'); after ~1970, 2–6-year (D') and 11–16-year (E') bands
- > NAO: before ~1970, 4.5–6.6-year band (C<sub>2</sub>'); after ~1970, 8.3–10.6-year band (E<sub>2</sub>'). NAO is also characterised by powerful short-term structures;
- > PDO: it is characterised by a longer-term variability (19.2–26.3-year band G). A 5.2–7.1-year band (C') is clearly expressed before ~1970 and disappears afterwards.

The time scales of the observed energy bands are given in Table III along with those detected in streamflow. A more accurate description of the spectral modes of these climate indices can be found in many other works such as Fernandes *et al.* (2003), Garcia *et al.* (2005), Massei *et al.* (2007), Coulibaly and Burn (2004), Torrence and Compo (1998), etc.

Local wavelet spectra of annual precipitation time series (Figure 4) clearly display very similar features that could be observed in streamflow and climate indices. Major spectral components and discontinuities

are detected such as 8–16-year and 3–6-year bands present in West/East North Central precipitation and Missouri/Upper Mississippi series, high power at 3–6-year around 1950 and between 1975 and 1990 in central precipitation as detected in Ohio streamflow (band D). The same ~1970 discontinuity is observed as well.

## 5.2. Relation between climate fluctuations and streamflow instationarity

Some general patterns and changes affecting climate indices are recovered in long-term fluctuations of streamflow. Although wavelet coherence would undoubtedly help in determining the intensity of correlation between the climatic and streamflow signals analysed, this approach was not used here because the time step for streamflow series and climate indices was basically not the same (respectively daily and monthly), which would have required streamflow to be downsampled according to a monthly time step. However, a detailed study of wavelet coherence would add some value, especially for the comparison of streamflow with several (more than three, as used in this study) climate indicators.

The change point around 1970 seems to be a constant pattern for precipitation, streamflow and climate index time series. Also, similar energy bands may be recovered (Figures 3 and 4, Table III). This characteristic time discontinuity was also reported by other works in unregulated watersheds (McCabe and Wolock, 2002; Anctil and Coulibaly, 2004; Coulibaly and Burn, 2004), which would then suggest a climatic rather than an anthropogenic origin of such a transient pattern. Here we demonstrate that this change point is associated with two major effects in streamflow according to the watershed considered:

1. It involves a shift in the inter- to pluri-annual band (in chronologic order: C, D, B) for Lower Mississippi, Upper Mississippi, Missouri and Arkansas (Figure 3). The (C, D, B) energy bands span the range of scales 2–8 years, which is also typical of SOI (Table III).
2. It involves the occurrence of an 8–16-year band (E) in Upper Mississippi and Missouri.

Although the 1970 change point and energy band D were detected in Ohio streamflow, this watershed is clearly apart from the others in terms of long-term inter-annual to pluri-annual fluctuations. We can also notice that it appears rather difficult to relate the power attenuation over the 1-year band with climate indices or precipitation variability, although it is particularly well marked for Arkansas, Upper Mississippi and Missouri.

SOI in particular appeared to display very similar modes of variability as those detected in the streamflow time series, especially in the case of Upper Mississippi and Missouri streamflow (Figure 3, bands E, C, D, B and C', E', D'), which deserves particular attention here. A global wavelet spectrum, gathering power across all the temporal range like a Fourier spectrum, was performed on these series to better compare the spectral

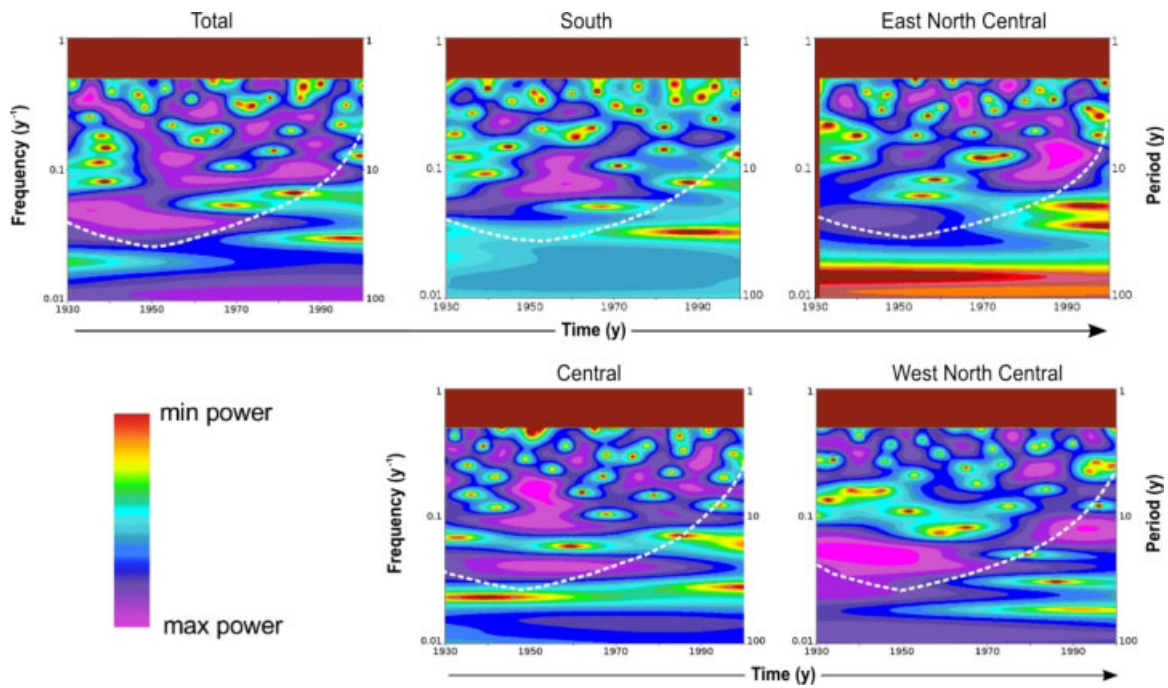


Figure 4. Continuous local wavelet spectra of annual precipitation time series. All purple contours are at least 90% significant when tested by the Monte Carlo simulation against a background red noise  $AR(1) = 0.98$ . This figure is available in colour online at [wileyonlinelibrary.com/journal/joc](http://wileyonlinelibrary.com/journal/joc)

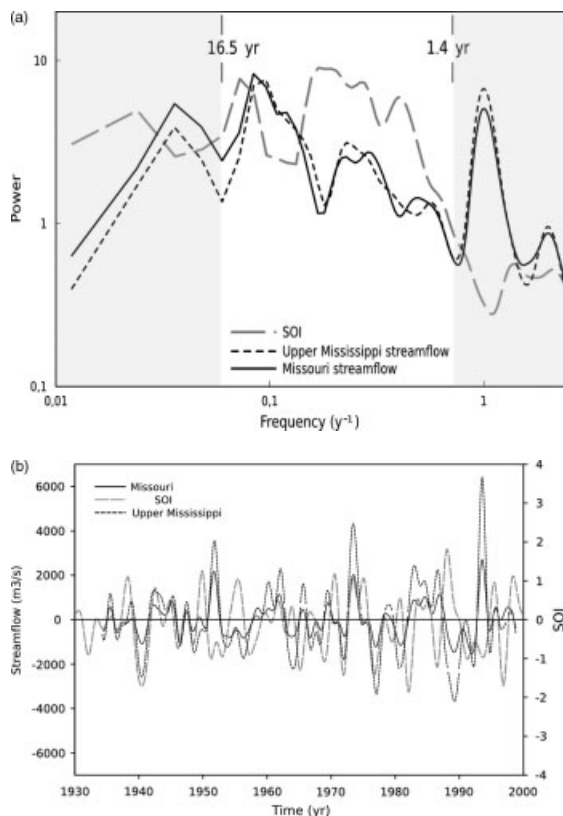


Figure 5. (a) Global wavelet spectra of SOI, Upper Mississippi and Missouri streamflow time series; (b) time-domain reconstructions of SOI, Upper Mississippi and Missouri streamflow 1.4–16.5-year energy bands.

components (Figure 5a). Upper Mississippi and Missouri spectra display clear similarities with the SOI spectrum

in the frequency range corresponding to the 1.4–16.5-year time scales. A shift in the spectrum towards higher frequencies is characteristic of a modulation by a high-frequency bearing signal: here it would provide evidence of a strong influence of SOI on Upper Mississippi and Missouri, i.e. on the Mississippi watershed headwaters in the 1.4–16.5-year scale range. It is difficult at this point to draw hypotheses on what physical mechanism would be involved in the filtering of the climate signal in Mississippi headwaters streamflow (atmospheric processes, anthropogenic impact...). Although the global wavelet spectra revealed a shift in the frequency of the streamflow in the 1.4–16.5-year band compared to the same band in SOI, it would be rewarding to compare the corresponding time-domain bands between streamflow and SO. The purpose of reconstruction is to check for similarity between the detected oscillations in SO and in streamflow (not between the two streamflow series) in terms of the expected physical influence: Do negative SOI values correspond to above-normal streamflow for that component that could possibly link SO and streamflow? A reconstruction of the 1.4–16.5-year band for Upper Mississippi, Missouri streamflow and SOI by inverse wavelet transform (Figure 5b) tend to show an overall good match between SOI and streamflow oscillations for the periods  $\approx 1934$ –1950 and  $\approx 1970$ –1985. This is consistent with the fact that positive ENSO phases (negative SOI phases) are associated with drier conditions in this region of the United States and the converse is also true. On the other hand, the  $\approx 1950$ –1970 and  $\approx 1985$ –1998 periods are characterised by a poorer correspondence between SOI and streamflow, which can be related to the temporal changes in the spectral composition described previously

in wavelet spectra (Figure 3). In all of the events, further physical interpretations would require many additional investigations.

From a quantitative standpoint, it is interesting to provide information about the part of variance associated with the various observed time scales. This can be achieved by wavelet scale averaging. Averaging in scale consists of extracting the power of a given energy band for a time series to either check for power variation through time or obtain the variance of the corresponding band relating to the total variance of the series. In our case, the issue to be addressed was the contribution of short-term (inferior to the synoptic maximum), annual and inter-/pluri-annual fluctuations of the total streamflow variance. We then computed scale-averaged wavelet spectra (not shown here) over the corresponding energy bands (Table IV). Three scale-averaged wavelet spectra were computed: the first spanning the range of short time scales inferior to the synoptic maximum, the second corresponding to the annual fluctuation power and the third corresponding to inter-/pluri-annual fluctuations. The time interval chosen for power integration was 3 months, which could preserve power variability associated with seasonal fluctuation. Each scale-averaged wavelet spectrum consisted of a 259 point-time series. The part of variance of the different energy bands is expressed as a percentage of the overall variance of each time series. The annual fluctuation obviously represents a large part of total power for each streamflow time series. However, in the long term, Upper Mississippi and Missouri display a strong power probably related to SOI variations as discussed above, whereas the overall Mississippi streamflow series (Lower Mississippi) and Ohio are definitely dominated by the annual oscillation. The strong power at the annual time scale in the lower Mississippi and Ohio compared to Upper Mississippi and Missouri cannot be explained here. One potential research track to be explored would concern the lower number of large dams with respect to the total basin area observed for the Missouri River compared to the others; for instance, the Missouri River comprises 581 large dams for an area of 1 331 810 km<sup>2</sup>, while Ohio comprises 711 for 490 603 km<sup>2</sup>. An attenuation of longer-term components, enhancing the variability associated with the annual cycle, could be a question that would require further investigations.

In the short term, Ohio, Arkansas and Missouri present the strongest contribution of high-frequency events compared to Lower and Upper Mississippi (2.9

and 1.1% respectively). Finally, summing the percentage of variance explained by high-frequency, annual and inter-/pluri-annual fluctuations for each series shows that Arkansas, with less than 40% of variance explained by powerful well-individualised components, is the more poorly structured time series, the remaining variance being explained by more or less noisy structures in the streamflow signal.

## 6. Long-term evolution of short-time flood events

One challenging concern lies in the link between high-frequency/extreme events (rain events, storms, depressions and other synoptic events...) and long-term variability. Jain and Lall (2001) investigated the potential impact of quasi-periodic, inter-annual and inter-decadal variations in climate (e.g. the ENSO) on flood frequency and reported a clear control of climate on floods. In this section, we try to investigate a possible control of long-term climate-driven oscillations on the short-term behaviour of the streamflow time series. In addition, the overall evolution in the power of high-frequency bands of streamflow is statistically tested to assess the temporal evolution of flood events over the 64-year period of study.

Scale-averaged wavelet spectra in Figure 6 are produced by scale averaging over the so-called synoptic band determined by the Fourier spectral analysis (i.e. the breakup time scale, approximately less than 30 days). The corresponding distribution of variance through time highlighted a statistically significant increase in the contribution of short-term fluctuations for Ohio, Upper Mississippi and Missouri (Figure 6). In order to investigate the possible modulations of these short-term time scales, that is, inferior to the synoptic maximum, by larger-scale climate fluctuations, we proceeded to a smoothing of all scale-averaged spectra using a Savitzky-Golay polynomial low-pass filter (Figure 7). This method is based on least squares polynomial fitting across a moving window within the data. It presents the advantage of preserving the higher moments in time-domain spectral peak data. The parameters of the filter chosen here were a fourth-order polynomial and a 2-year width smoothing window, which offered the best trade-off between variance conservation and smoothing.

For all time series, the smoothed scale-averaged wavelet spectra revealed an obvious modulation by larger time scales, in particular by a  $\approx 2$ –4-year fluctuation (Figure 7). This time scale is typical of some well-known

Table IV. F-statistics and associated *p*-values for increasing trend of each reconstructed climate-related component.

	Lower Mississippi	Arkansas	Ohio	Upper Mississippi	Missouri
% of total variance for time scales < synoptic max.	2.9	4.8	6.4	1.1	4.7
% of total variance for annual fluctuation	48.6	19.1	45.3	30.8	19.2
% of total variance for inter-annual/pluri-annual fluctuations	11.5	16.0	6.6	25.3	26.0
Sum of < synoptic max., annual and inter/pluriannual (%)	63.0	39.9	58.3	57.2	49.9

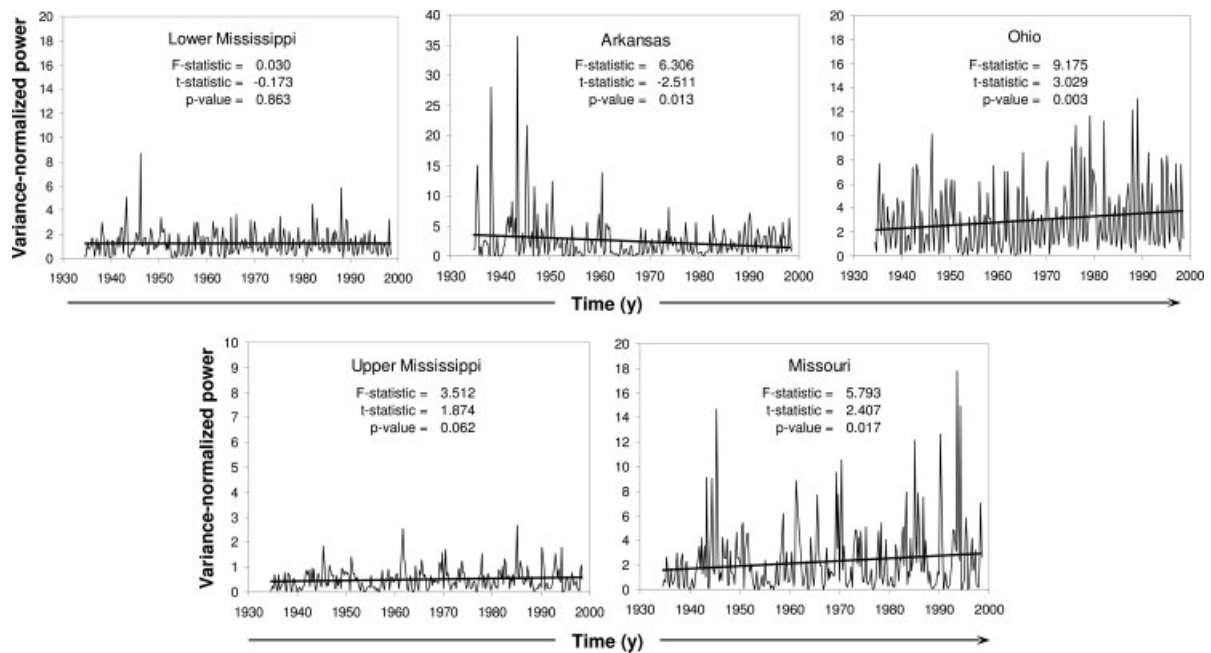


Figure 6. Scale-averaged wavelet spectra of short-term streamflow fluctuations. The short-term time scale limit was chosen according to Fourier spectra ( $\beta_1$  scaling exponent), and one seeks possible trends in meteorologic-induced short-time events such as floods. Linear regression models and slopes are statistically tested by ANOVA (F-statistic) and Student  $t$ -test ( $t$ -statistic) respectively.

climate indices' fluctuations such as the SOI/ENSO, as described in Section 5 above, which is known to display a particularly strong power since approximately 1960 (Torrence and Compo, 1998). This would suggest a significant control of large-scale climate on the most rapid fluctuations in streamflow. The discontinuity that could be observed on the local wavelet spectra starting around the mid-1950s (see Section 5.1) was observed on the smoothed scale-averaged spectra, which was barely visible on the initial scale-averaged spectra (Figure 6) except for Arkansas. After this mid-1950s' discontinuity, all smoothed spectra but those of lower and Upper Mississippi displayed a statistically significant increase in the power of high-frequency streamflow, which means that the contribution in terms of amplitude of short-term events to the total discharge tends to become greater. A flood frequency analysis should be conducted additionally to test the hypothesis of an associated increase in their number.

## 7. Conclusion

In this study, Mississippi and tributaries streamflow series were used to investigate long-term to short-term streamflow variability in relation with climate fluctuations. Two main issues were initially addressed (i) the identification of the nature and the temporal characteristics of long-term fluctuations and the quantification of their influence in streamflow variability and (ii) the behaviour of streamflow regarding short-term fluctuations related to meteorologic events (of the order of 15 to 25 days) such as strong floods: Are they linked to longer-term climate patterns, of what type/nature? Do they present a significant trend throughout the last 64 years?

All streamflow time series exhibited statistically significant increasing trends. A major change point was observed in streamflow around 1970. This change point, also reported in many other works, would affect most of the spectral components, and is characterised by the occurrence of a powerful 8–16-year band for both Upper Mississippi and Missouri Rivers, and of a 3–6-year band for all rivers. It has been shown that this discontinuity is also a characteristic pattern of all selected climate indices (SOI, PDO, NAO). Also, a lack of power affecting more specifically the annual band between approximately 1955 and 1975 was detected to be more pronounced for Arkansas, Upper Mississippi and Missouri, which would occur almost simultaneously with another temporal discontinuity starting in the mid-1950s; however, no link could be established between these two phenomena. It may be rewarding in further investigations to search for possible links between this 1-year band power attenuation and major periods of dam construction. Finally, a last change starting around 1985 was detected in streamflow series. It was difficult to relate the energy bands observed in climate indices and in streamflow, except between SOI and Upper Mississippi and Missouri. For those basins, a potentially strong link was deduced in the 1.4–16.5-year range, which appeared rather consistent from a physical standpoint after time-domain reconstruction of this mode of variability in each series. A wavelet coherence analysis involving climate indices, precipitation and the same streamflow series, currently carried out as a continuity of this work, will certainly constitute a most appropriate approach to the quantification of climate-originating modes in streamflow variability.

The contribution of inter-annual to pluri-annual oscillations ranged from 6.6 to 26% of the total streamflow

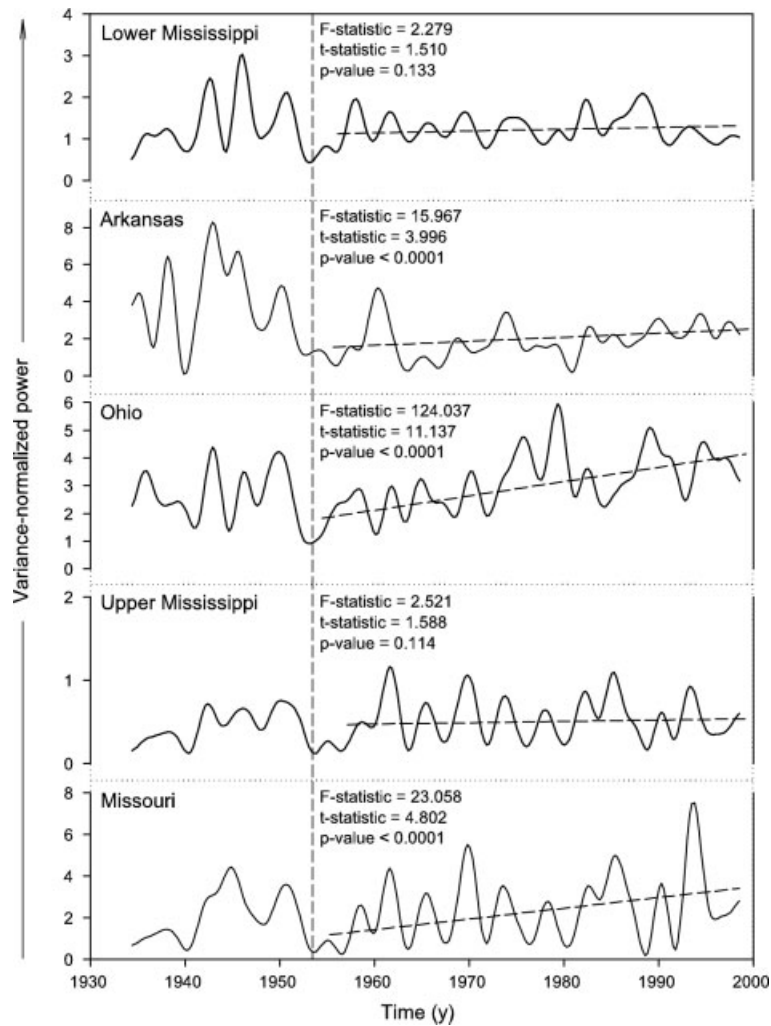


Figure 7. Stavitsky–Golay fourth-order polynomial smoothing of scale-averaged wavelet spectra presented in Figure 4. The smoothing procedure reveals (1) a possible modulation of short-term fluctuations by a quasi-biennial fluctuation (less expressed for Arkansas and Ohio) and (2) a time discontinuity beginning around about 1953, after which high-frequency streamflow increases significantly and seems to be more controlled by a quasi-biennial climate fluctuation.

variance. In the short term, i.e. for time scales related to synoptic activity ( $>2$ – $3$  weeks), high-frequency fluctuations explained from 1.1 to 6.4% of the total streamflow variance. The annual cyclicality was more or less well expressed in streamflow variability according to each watershed, from 19.1 to 48.6%. High-frequency streamflow fluctuations linked to synoptic activity were also found to increase after 1955 for all basins except Upper Mississippi and Lower Mississippi (i.e. the whole Mississippi basin). Finally, a control of short-term streamflow variations by larger-scale climate fluctuations was demonstrated in the form of a modulation by a  $\approx 2$ – $4$ -year fluctuation.

## References

- Ancil F, Coulibaly P. 2004. Wavelet analysis of the interannual variability in southern Québec streamflow. *Journal of Climate* **17**: 163–173.
- Coulibaly P, Burn D. 2004. Wavelet analysis of variability in annual Canadian streamflows. *Water Resources Research* **40**: W03105, DOI:10.1029/2003WR002667.
- Fernandez I, Hernandez CN, Pacheco JM. 2003. Is the North Atlantic Oscillation just a pink noise? *Physica A* **323**: 705–714.
- Garcia NO, Gimeno L, De La Torre L, Nieto R, Anem JA. 2005. North Atlantic Oscillation (NAO) and precipitation in Galicia (Spain). *Atmosfera* **1**: 25–32.
- Guttman NB, Quayle RG. 1996. A historical perspective of U.S. climate divisions. *Bulletin of the American Meteorological Society* **77**(2): 293–303.
- Hanson RT, Dettinger MD, Newhouse MW. 2006. Relations between climatic variability and hydrologic time series from four alluvial basins across the southwestern United States. *Hydrogeology Journal* **14**(7): 1122–1146, DOI:10.1007/s10040-006-0067-7.
- Hurrell J, Kushnir Y, Ottersen G, Visbeck M. 2003. The North Atlantic Oscillation: Climatic Significance and Environmental Impact. *Geophysical monograph (American Geophysical Union)* **134**: 1–35.
- Jain S, Lall U. 2001. Floods in a changing climate: does the past represent the future? *Water Resources Research* **37**(12): 3193–3205.
- Jha M, Arnold JG, Gassman PW, Giorgi F, Gu RR. 2006. Climate change sensitivity assessment on Upper Mississippi River Basin streamflows using SWAT. *Journal of the American Water Resources Association* **42**(4): 997–1015.
- Jha M, Pan ZT, Takle ES, Gu R. 2004. Impacts of climate change on streamflow in the Upper Mississippi River Basin: A regional climate model perspective. *Journal of Geophysical Research* **109**: D09105, DOI:10.1029/2003JD003686.
- Labat D. 2005. Recent advances in wavelet analysis: part 1. A review of concepts. *Journal of Hydrology* **314**: 275–288.

- Labat D, Ronchail J, Guyot JL. 2005. Recent advances in wavelet analyses: part 2 – Amazon, Parana, Orinoco and Congo discharges time scale variability. *Journal of Hydrology* **314**(1–4): 289–311.
- Lins HF, Slack JR. 1999. Streamflow trends in the United States. *Geophysical Research Letters* **26**(2): 227–230.
- McCabe GJ, Palecki MA, Betancourt JL. 2004. Pacific and Atlantic Ocean influences on multidecadal drought frequency in the United States. *Proceedings of the National Academy of Sciences* **101**(12): 4136–4141.
- McCabe GJ, Wolock DM. 2002. A step increase in streamflow in the conterminous United States. *Geophysical Research Letters* **29**(24): 2185.
- Massei N, Durand A, Deloffre J, Dupont JP, Valdes D, Laignel B. 2007. Investigating possible links between the North Atlantic Oscillation and rainfall variability in northwestern France over the past 35 years. *Journal of Geophysical Research* **112**: D09121, DOI:10.1029/2005JD007000.
- Mauget S. 2004. Low frequency streamflow regimes over the central United States: 1939–1998. *Climatic Change* **63**: 121–144.
- Nijssen B, O'donnell GM, Hamlet AF, Lettenmaier DP. 2001. Hydrologic sensitivity of global rivers to climate change. *Climatic Change* **50**: 143–175.
- Novotny EV, Stefan HG. 2007. Stream flow in Minnesota: indicator of climate change. *Journal of Hydrology* **334**(3–4): 319–333.
- Pagano T, Garen D. 2005. A recent increase in western U.S. streamflow variability and persistence. *Journal of Hydrometeorology* **6**: 173–179.
- Schneider K, Farge M. 2006. Wavelets: theory. In *Encyclopedia of Mathematics Physics*, Françoise JP, Naber G, Tsu TS (eds). Elsevier, 426–437.
- Stewart IT, Cayan DR, Dettinger MD. 2005. Changes toward Earlier Streamflow Timing across Western North America. *Journal of Climate* **18**: 1136–1155.
- Torrence C, Compo GP. 1998. A practical guide to wavelet analysis. *Bulletin of the American Meteorological Society* **79**: 61–78.
- Walling DE, Fang D. 2003. Recent trends in the suspended sediment loads of the world's rivers. *Global and Planetary Change* **39**(1–2): 111–126.
- Ziegler AD, Maurer EP, Sheffield J, Nijssen B, Wood EF, Lettenmaier DP. 2005. Detection time for plausible changes in annual precipitation, evapotranspiration, and streamflow in three Mississippi River sub-basins. *Climatic Change* **72**(1–2): 17–36.